High-Temperature and Low-Frequency Acoustic Energy Absorption by a Novel Porous Metamaterial Structure**

Qihang Liu[1]   Xuewei Liu[2]   Chuanzeng Zhang[1]*   Fengxian Xin[2]

([1]*Department of Civil Engineering, University of Siegen, Siegen 57076, Germany*)
([2]*State Key Laboratory for Strength and Vibration of Mechanical Structures, Xi'an Jiaotong University, Xi'an 710049, China*)

© The Author(s) 2021

ABSTRACT In this paper, we propose a novel porous metamaterial structure with an improved acoustic energy absorption performance at high-temperature and in the low-frequency range. In the proposed novel porous metamaterial structure, a porous material matrix containing periodically perforated cylindrical holes arranged in a triangular lattice pattern is applied, and additional interlayers of another porous material are introduced around these perforations. The theoretical model is established by adopting the double porosity theory for the interlayer and the cylindrical hole which form an equivalent inclusion and then applying the homogenization method to the porous metamaterial structure formed by the equivalent inclusion and the porous matrix. The temperature-dependent air and material parameters are considered in the extended theoretical model, which is validated by the finite element results obtained by COMSOL Multiphysics. The acoustic or sound energy absorption performance can be improved remarkably at very low frequencies and high temperature. Furthermore, the underlying acoustic energy absorption mechanism inside the unit-cell is investigated by analyzing the distribution of the time-averaged acoustic power dissipation density and the energy dissipation ratio of each constituent porous material. The results reveal that regardless of the temperature, the acoustic energy is mostly dissipated in the porous material with a lower airflow resistivity, while the acoustic energy dissipated in the porous material with a higher airflow resistivity also becomes considerable in the high-frequency range. The novel porous metamaterial structure proposed in this paper can be efficiently utilized to improve the acoustic energy absorption performance at high temperature.

KEY WORDS Novel porous metamaterial structure, Double porosity theory, Homogenization method, Acoustic or sound energy absorption, High temperature

1. Introduction

Energy-absorbing materials and structures [1–3] are widely used in engineering applications to provide an adequate mechanical or thermal protection [4] and reduce harmful noises [5–8]. Besides the design of highly efficient energy-absorbing structures, such as the acoustic black holes (ABHs) which show great potential in impact protection, vibration attenuation and noise reduction [9–12], the proper selection of highly energy-absorbing materials is also essential. Porous materials composed of

---

* Corresponding author. E-mail: c.zhang@uni-siegen.de

** This paper is dedicated to Professor Tongxi Yu (The Hong Kong University of Science and Technology, China) on the occasion of his 80th birthday.

randomly distributed micro-pores are highly effective for mechanical and acoustic energy absorption. In order to describe the acoustic or sound energy absorption characteristics of such materials, analytical models for porous materials with simple pore morphologies such as parallel cylindrical or slit-like pores were first proposed by Zwikker and Kosten [13] in 1949, in which the dynamic mass density and bulk modulus were calculated under the assumption of rigid and motionless skeletons. Then purely empirical models [14, 15] were developed using power-law functions dependent on the static airflow resistivity to describe the complex wave number and characteristic impedance. For more complicated pore morphologies, semi-phenomenological models such as the Johnson-Champoux-Allard (JCA) model [16, 17] were proposed with five parameters involving not only the static airflow resistivity and porosity, but also the tortuosity and viscous characteristic length for describing the viscous effect, and the thermal characteristic length for considering the thermal effect. Later on, Pride et al. [18] and Lafarge [19] further modified the JCA model for calculating the dynamic mass density and bulk modulus with a higher accuracy, which, however, are rather complicated because they require more parameters which are difficult to measure.

However, conventional porous materials only have an effective sound energy absorption performance with a quite large bandwidth at relatively high frequencies in general. For improving their low-frequency absorption capability, in the past few decades, scientists began to work on the double porosity materials which have two interconnected pores of very different characteristic sizes. The homogenization method [20] was proposed and employed for the study of the sound energy absorption of double porosity materials with periodically distributed perforations [21–23] or periodically arranged slits [24–26]. Besides, porous composite materials with inclusions and composite porous metamaterials were also investigated, and it was demonstrated that such materials are also highly capable of enhancing the sound energy absorption performance [27–30].

In addition to the above-mentioned research work at room temperature, porous materials have also been used for sound energy absorption in high-temperature environments such as in the combustion chambers of gas turbines [31]. In such cases, the air and material properties vary considerably with the change of temperature, and they should be designed properly to match the extreme high-temperature conditions. Therefore, the high-temperature sound energy absorption characteristics of porous materials have been analyzed comprehensively in the past years. Since the static airflow resistivity plays a critical role in most of the established models for porous materials, its dependence on temperature was first estimated by Christie [32] through experiments and further verified by Williams et al. [33] Sun et al. [34] studied the high-temperature effects on the acoustic parameters of fibrous metal materials by thermodynamics and heat transfer theory considering the temperature-dependent material properties. Furthermore, the surface-specific acoustic impedances and the acoustic absorption coefficients for normal incidence were also investigated theoretically and experimentally. Ren et al. [35] developed a semi-analytical model from the microscopic perspective and analyzed the influence of temperature on acoustic wave or sound propagation in sintered metal fiber materials by considering the variations of thermal parameters of saturated air with temperature.

In spite of the above-mentioned previous studies, however, the acoustic or sound energy absorption performance of conventional porous materials at high temperature still needs to be further improved, especially in the low-frequency range. Therefore, a new kind of porous metamaterial structure is proposed in this paper. The proposed novel porous metamaterial structure is composed of three components, namely, a porous material as matrix, periodically perforated cylindrical holes arranged in a triangular lattice pattern, and another porous material as interlayers between the porous matrix and the perforated cylindrical holes. The introduction of additional interlayers consisting of another porous material around the perforations aims to form a novel porous metamaterial or composite structure by combining the advantages of the two different constituent porous materials (inner porous material interlayer and outer porous material matrix) and to obtain an improved sound energy absorption performance at high temperature, in the low-frequency range and with a sufficiently large bandwidth. A theoretical model for the proposed novel porous metamaterial structure is established, and its sound energy absorption characteristics are analyzed by taking the temperature-dependent air and material parameters into consideration. The established theoretical model is then validated by the finite element (FE) software COMSOL Multiphysics. To reveal the underlying acoustic or sound energy absorption mechanism inside the unit-cell of the porous metamaterial structure, the distributions of

the time-averaged acoustic power dissipation density in the unit-cell and the energy dissipation ratio of the two constituent porous materials at different temperatures are studied and discussed in details. Finally, some conclusions are drawn, which are relevant for the design, optimization and application of the proposed novel porous metamaterial structure at low frequencies and in the high-temperature environments.

2. Theoretical and Numerical Models

2.1. Theoretical Model

Let us consider a porous metamaterial or composite structure as shown in Fig. 1a, which is composed of a porous material (material 2) as matrix, periodically perforated cylindrical holes arranged in a triangular lattice pattern, and another porous material (material 1) as interlayers between the matrix and the perforations. It should be noted here that the present study focuses on the triangular lattice pattern of the perforated cylindrical holes, though other arrangements or lattice pattern of the perforated cylindrical holes can also be considered. The porous metamaterial structure is subjected to a normally incident acoustic wave. Due to the periodicity of the cylindrical perforations, a hexagonal unit-cell is used to represent the sound energy absorption characteristics of the whole porous metamaterial structure. To simplify the analysis, the hexagonal unit-cell is approximated by a cylindrical unit-cell having the same volume. The cylindrical unit-cell can be considered as a porous matrix (material 2) containing an equivalent acoustic inclusion, which is a double porosity material consisting of the cylindrical perforation and the porous interlayer (material 1). The radius of the unit-cell is r_2, the perforation radius is R_p, the thickness of the inner porous material interlayer is $r_2 - r_1$, and h denotes the height of the unit-cell. In the following analysis, the subscript m is used to represent the acoustic parameters related to the porous materials and the parameters with the subscript p represent the parameters of the perforation. The subscript dp denotes the double porosity material, and the quantities without any subscripts apply for the entire unit-cell.

Both porous materials 1 and 2 used in our porous metamaterial structure are described by the JCA model [16, 17], which is a semi-phenomenological model used to describe the equivalent dynamic mass density and bulk modulus of an acoustical porous material having arbitrary pore shapes. Five parameters are involved in the JCA model, namely, the porosity, the static airflow resistivity, the tortuosity factor, the viscous characteristic length, and the thermal characteristic length. The static airflow resistivity and the tortuosity factor can characterize the visco-inertial effects, and the latter can be considered as a measure of the disorder in the material. The viscous characteristic length describes the viscous effects, while the thermal characteristic length describes the thermal effects, and both of them can be estimated from the standing wave tube measurements or ultrasound techniques [36–38]. Based on the JCA model, the equivalent dynamic mass density and bulk modulus for the two porous materials in our porous metamaterial structure can be expressed as

$$\rho_{mi} = \frac{\alpha_{\infty mi}\rho_0}{\phi_{mi}}\left[1 + \frac{\sigma_{mi}\phi_{mi}}{j\omega\rho_0\alpha_{\infty mi}}\sqrt{1 + j\frac{4\alpha_{\infty mi}^2\eta\rho_0\omega}{\sigma_{mi}^2\Lambda_{mi}^2\phi_{mi}^2}}\right] \quad (i = 1, 2) \tag{1}$$

$$K_{mi} = \frac{\gamma P_0/\phi_{mi}}{\gamma - (\gamma - 1)\left[1 - j\frac{8\kappa}{\Lambda_{mi}'^2 C_p\rho_0\omega}\sqrt{1 + j\frac{\Lambda_{mi}'^2 C_p\rho_0\omega}{16\kappa}}\right]^{-1}} \quad (i = 1, 2) \tag{2}$$

where $j = \sqrt{-1}$ is the imaginary unit, ω is the angular frequency, $\varphi_{mi}, \sigma_{mi}, \alpha_{\infty mi}, \Lambda_{mi}$ and Λ_{mi}' are the porosity, static airflow resistivity, tortuosity factor, viscous, and thermal characteristic lengths of the two porous materials, respectively, ρ_0 and η are the mass density and dynamic viscosity of air, P_0 is the ambient pressure, C_p is the specific heat capacity of air at constant pressure, γ is the specific heat ratio, and κ is the heat conductivity of air. The subscript $i = 1, 2$ in Eqs. (1) and (2) designates the porous materials 1 and 2, respectively.

For the cylindrical perforation, the porosity is defined by $\phi_{p1} = R_p^2/r_1^2$. The equivalent dynamic mass density and the equivalent dynamic bulk modulus of a material with a cylindrical hole of circular cross section can be expressed as [13]

$$\rho_p = \frac{\rho_0}{\phi_{p1}} \times 1 \Big/ \left[1 - \frac{2}{\beta\sqrt{-j}} \frac{J_1\left(\beta\sqrt{-j}\right)}{J_0\left(\beta\sqrt{-j}\right)}\right] \tag{3}$$

$$K_p = \frac{P_0}{\phi_{p1}} \times \gamma \Big/ \left[1 + (\gamma - 1)\frac{2}{\beta\sqrt{-j\,\mathrm{Pr}}} \frac{J_1\left(\beta\sqrt{-j\,\mathrm{Pr}}\right)}{J_0\left(\beta\sqrt{-j\,\mathrm{Pr}}\right)}\right] \tag{4}$$

where $\beta = \bar{r}\sqrt{\frac{\omega\rho_0}{\eta}}$, $\bar{r}$ is the so-called hydraulic radius which equals to R_p, $\mathrm{Pr} = \eta C_p/\kappa$ is the Prandtl number, and J_i represents the Bessel function of the first kind and i-th order.

The dynamic mass density and bulk modulus of the perforated porous material consisting of the cylindrical hole and the inner porous material (porous material 1) interlayer can be obtained by the double porosity theory [22] as

$$\rho_{dp} = \left[\frac{1}{\rho_p} + (1 - \phi_{p1})\frac{1}{\rho_{m1}}\right]^{-1} \tag{5}$$

$$K_{dp} = \left[\frac{1}{K_p} + (1 - \phi_{p1})\frac{F_{d1}\left(\omega\frac{P_0}{\phi_{m1}K_{m1}}\right)}{K_{m1}}\right]^{-1} \tag{6}$$

where $F_{d1}\left(\omega\right)$ is introduced to describe the dissipative effect of the pressure diffusion, which can be expressed as

$$F_{d1}(\omega) = 1 - j\frac{\omega}{\omega_{d1}}\frac{D_1\left(\omega\right)}{D_1\left(0\right)} \tag{7}$$

in which $\omega_{d1} = (1 - \phi_{p1})P_0/\phi_{m1}\sigma_{m1}D_1(0)$ is the characteristic frequency of the pressure diffusion effect. A semi-phenomenological expression for $D_1\left(\omega\right)$ in Eq. (7) is given by [22, 39]

$$D_1(\omega) = \frac{D_1(0)}{j\frac{\omega}{\omega_{d1}} + \sqrt{1 + j\frac{M_{d1}}{2}\frac{\omega}{\omega_{d1}}}} \tag{8}$$

where $D_1(0)$ is defined by [39]

$$D_1(0) = \frac{r_1^2}{4}\left(\ln\left(\frac{1}{\phi_{p1}}\right) - \frac{3}{2} + 2\phi_{p1} - \frac{\phi_{p1}^2}{2}\right) \tag{9}$$

and the form parameter M_{d1} is determined by [22]

$$M_{d1} = \frac{8D_1(0)}{\Lambda_{d1}^2(1 - \phi_{p1})} \tag{10}$$

in which

$$\Lambda_{d1} = \frac{2h\left(\pi r_1^2 - \pi R_p^2\right)}{2\pi h R p + \pi r_1^2 - \pi R_p^2} \tag{11}$$

It is noted here that $F_{d1}(\omega)$ in Eq. (6) should be replaced by 1 if $\omega \ll \omega_{VM1}$ and $\omega_{d1} \ll \omega_{VM1}$ are not satisfied, where $\omega_{VM1} = \sigma_{m1}\phi_{m1}/(\rho_0\alpha_{\infty m1})$ is the cutoff angular frequency. In this case, the airflow participates in both the micro-pore domain of the porous material and the cylindrical hole, and the acoustic pressure is distributed homogeneously along the direction of the acoustic wave propagation.

Since the unit-cell can be considered as an equivalent inclusion of a double porosity material (porous material 1 and cylindrical hole) embedded in a porous matrix (porous material 2), the dynamic mass density and the dynamic bulk modulus of the whole unit-cell can be deduced by the homogenization method as [22]

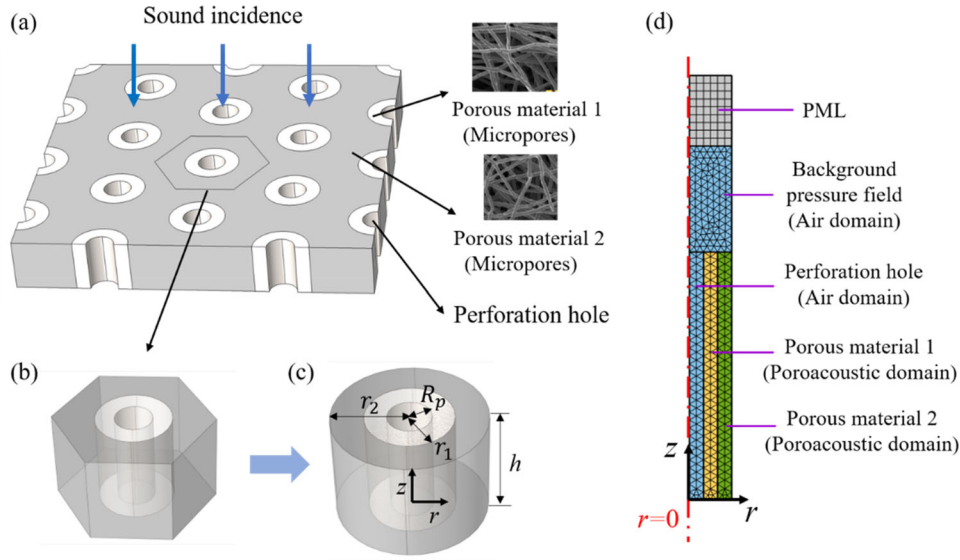$$\rho = \left[\frac{\phi_{p2}}{\rho_{dp}} + (1 - \phi_{p2})\frac{1}{\rho_{m2}}\right]^{-1} \tag{12}$$

Fig. 1. **a** Acoustic wave propagation in a novel porous metamaterial structure; **b** hexagonal unit-cell; **c** approximate cylindrical unit-cell; **d** two-dimensional (2D) axisymmetric finite element model for the unit-cell

$$K = \left[\frac{\phi_{p2}}{K_{dp}} + (1 - \phi_{p2}) \frac{F_{d2}}{K_{m2}} \right]^{-1} \tag{13}$$

where $\phi_{p2} = r_1^2 / r_2^2$, and F_{d2} can be obtained by changing the subscript 1 to 2 in Eqs. (7)–(10), while Λ_{d2} is now given by

$$\Lambda_{d2} = \frac{2h \left(\pi r_2^2 - \pi r_1^2 \right)}{2\pi h r_1 + \pi r_2^2 - \pi r_1^2} \tag{14}$$

Once the equivalent dynamic mass density and bulk modulus of the unit-cell are obtained, the characteristic acoustic impedance and wave number can be calculated by

$$Z_c = (\rho K)^{1/2} \tag{15}$$

$$k = \omega \left(\rho / K \right)^{1/2} \tag{16}$$

With a rigid back, the surface impedance and sound absorption coefficient are determined by [40]

$$Z_s = -j Z_c \cot (kh) \tag{17}$$

$$\alpha = 1 - \left| \frac{Z_s - \rho_0 c_0}{Z_s + \rho_0 c_0} \right|^2 \tag{18}$$

where c_0 is the sound speed in air. The above theoretical model can be further extended to high-temperature conditions by applying the corresponding parameters of air and the porous materials at different temperatures.

2.2. Numerical Model

To validate the theoretical model described in the previous subsection and further investigate the sound energy absorption mechanism inside the unit-cell of the porous metamaterial structure, a two-dimensional (2D) axisymmetric finite element (FE) model is established using the commercial software COMSOL Multiphysics, which is shown in Fig. 1d. The red dash-dotted line represents the rotation axis of the 2D axisymmetric model, and all the other three sides are sound-hard boundaries. The cylindrical hole is considered as the air domain and both porous materials, i.e., porous matrix (porous material 2) and porous interlayer (porous material 1), are defined as the poroacoustic domains described by the JCA model. For generating the incident plane sound wave, a background pressure field is introduced as

Table 1. **Physical parameters of air at different temperatures**

t ($°C$)	ρ_0 (kg/m^3)	c_0 (m/s)	η (10^{-5}Pa$\cdot$s)	C_p (J/kg/K)	γ (1)	κ (10^{-2}W/m/K)
20	1.23	343	1.82	1006.4	1.402	2.55
100	0.94	387	2.19	1011.5	1.397	3.11
300	0.614	476	2.98	1045.4	1.379	4.37
500	0.456	549	3.66	1092.7	1.356	5.48

the air domain. A perfectly matched layer (PML) is attached to the top part of the air domain of the background pressure field to avoid acoustic wave reflections at the top boundary of the air domain of the background pressure field. Free triangular meshes are used for all the computational domains except the PML, where mapped meshes are applied. Besides, quadratic elements are employed in the whole simulation. In the present analysis, the minimum wavelength, which is defined by the ratio of the sound speed at room temperature to the sound frequency, increases with the increase of temperature as the sound speed in air also increases with the increase of temperature. Thus, the maximum mesh size for room temperature can be used for both room and high- temperature conditions. Our own experiences show that a maximum mesh size smaller than one-sixth of the minimum wavelength is sufficient to ensure the accuracy and convergence of the numerical model. For this reason, the maximum mesh size is chosen to be smaller than one-tenth of the minimum wavelength at room temperature in our calculations, which means that the used mesh resolves the smallest wavelength with 10 elements to ensure the accuracy and convergence of the numerical model. The used mesh can handle approximately a maximum frequency of 16666 Hz, which covers the frequency range of 0 to 2000 Hz considered in our analysis. With the abovementioned criteria for the mesh-size selection, the numerical model as shown in Fig. 1d consists of 441 elements and 279 degrees of freedom (DOFs) in total.

The surface impedance is computed by $Z_s = \langle p \rangle / \langle v \rangle$, where $\langle p \rangle$ and $\langle v \rangle$ are the average values of the sound pressure and normal velocity of the particles on the top surface of the unit-cell, respectively. Therefore, the sound absorption coefficient can be calculated by Eq. (18).

3. Temperature-Dependent Material Parameters

The above theoretical and numerical models can be further extended to high-temperature conditions by considering the corresponding temperature-dependent air and material parameters at different temperatures. Among the five parameters of the porous materials in the JCA model, only the static airflow resistivity σ varies significantly with temperature t [35] and its temperature dependence can be described by Christie's law [32]

$$\sigma = \sigma_0 \left(\frac{t + 273.15}{293.15} \right)^{0.6} \tag{19}$$

where σ_0 is the reference static airflow resistivity at the room temperature of $t_0 = 20°C$ or $t_0 = 293.15$K.

However, the physical parameters of air are highly dependent on temperature. The software REF-PROP of NIST can be applied to calculate the corresponding physical parameters of air for selected temperatures at the atmospheric pressure $P_0 = 101330$Pa based on numerous fitted curves of the experimental data, and these parameters are listed in Table 1.

4. Results and Discussion

The acoustic or sound energy absorption characteristics of the proposed porous metamaterial structure and the underlying physical mechanism are studied in detail in this section. In our calculations, the cylindrical unit-cell of the porous metamaterial structure has the following geometrical parameters: $R_p = 4$mm, $r_1 = 8$mm, $r_2 = 12$mm, and $h = 90$mm. Two porous materials made of sintered metal fibers and rockwool are selected and marked as Fib1 and Fib2, respectively, and their material parameters at the room temperature of 20°C are shown in Table 2. In the following analysis, the porous material Fib1 is taken as the inner porous interlayer and Fib2 as the outer porous matrix.

The sound absorption coefficient and surface impedance (normalized by the characteristic impedance of air) curves are shown in Fig. 2. It can be observed here that fairly good agreements
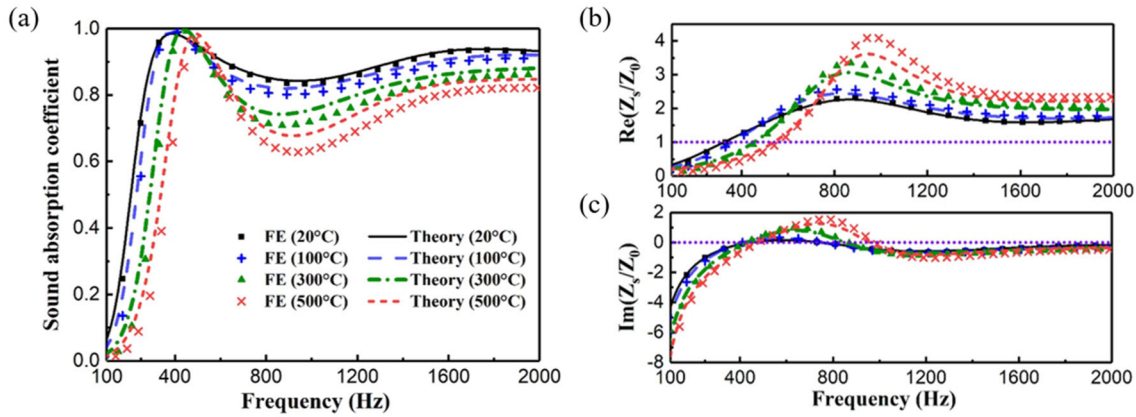
Fig. 2. **a** Sound absorption coefficient; **b** real part; **c** imaginary part of the normalized surface impedance curves at different temperatures

Table 2. **Material parameters at 20 °C**

Material	ϕ_{mi}	σ_{mi} $(\mathrm{N \cdot s \cdot m^{-4}})$	$\alpha_{\infty mi}$	Λ_{mi} (μm)	Λ'_{mi} (μm)
Fib1 (sintered metallic fibrous material)	0.90	12057	1.085	141	225
Fib2 (rockwool)	0.94	1,35,000	2.1	49	166

between the theoretical and numerical results are achieved, which validates the theoretical model established in the paper. At room temperature, the sound absorption coefficient is above 0.8 starting from a low frequency of about 270 Hz on, and the peak is located at around 390 Hz with a value of about 0.986. At 100°C, the sound absorption coefficient is above 0.8 from 290 Hz on, while at 300°C, the coefficient is above 0.7 from 340 Hz on. For a perfect sound energy absorber [41], it requires that the real part of the surface impedance of the structure (acoustic resistance) equals to that of air (i.e., $\mathrm{Re}(Z_s/Z_0) = 1$) and the imaginary part of the surface impedance (acoustic reactance) equals to zero (i.e., $\mathrm{Im}(Z_s/Z_0) = 0$). As temperature rises, the peak position only slightly shifts to a higher frequency by several dozens of Hz and the peak value always remains higher than 0.985, which can be explained by the good match of the surface impedance of the structure with the impedance of air. However, in the intermediate-frequency range, the acoustic resistance deviates farther away from 1 with the increase of temperature, which results in a poor match of the surface impedance with the impedance of air. Thus, the sound absorption coefficient decreases and a trough can be observed around 1000 Hz. Nevertheless, it can still be concluded that the sound energy absorption is sufficiently efficient at very low frequencies with a large bandwidth at high temperature.

To demonstrate the sound absorption performance of the novel porous metamaterial structure, the comparison of the sound absorption coefficients for the proposed metamaterial structure, the double porosity materials (porous materials with cylindrical holes), and the pristine porous materials without cylindrical holes or perforations having the same geometry is shown in Fig. 3. Here, Fib1 and Fib2 are used to represent the pristine porous materials without cylindrical holes, while DP-Fib1 and DP-Fib2 are used to represent the double porosity materials with cylindrical holes but without additional interlayers. It can be observed from Fig. 3 that for the two pristine porous materials without cylindrical holes, the sound absorption coefficients decrease significantly with the increase of temperature and become inefficient. Among the other three cases with cylindrical holes, a peak in the sound absorption coefficient is induced in the low-frequency range. At the same temperature, the peak value of the sound absorption coefficient for DP-Fib2 is smaller than that for the novel porous metamaterial structure and the one for the DP-Fib1, and it appears always at the lowest frequency. The peak value of the sound absorption coefficient for the novel porous metamaterial structure is comparable with that of DP-Fib1 at 20°C and 500°C, but higher than that for DP-Fib1 at 100°C and 300°C. The peak position of the sound absorption coefficient for the novel metamaterial structure only shifts slightly to a higher
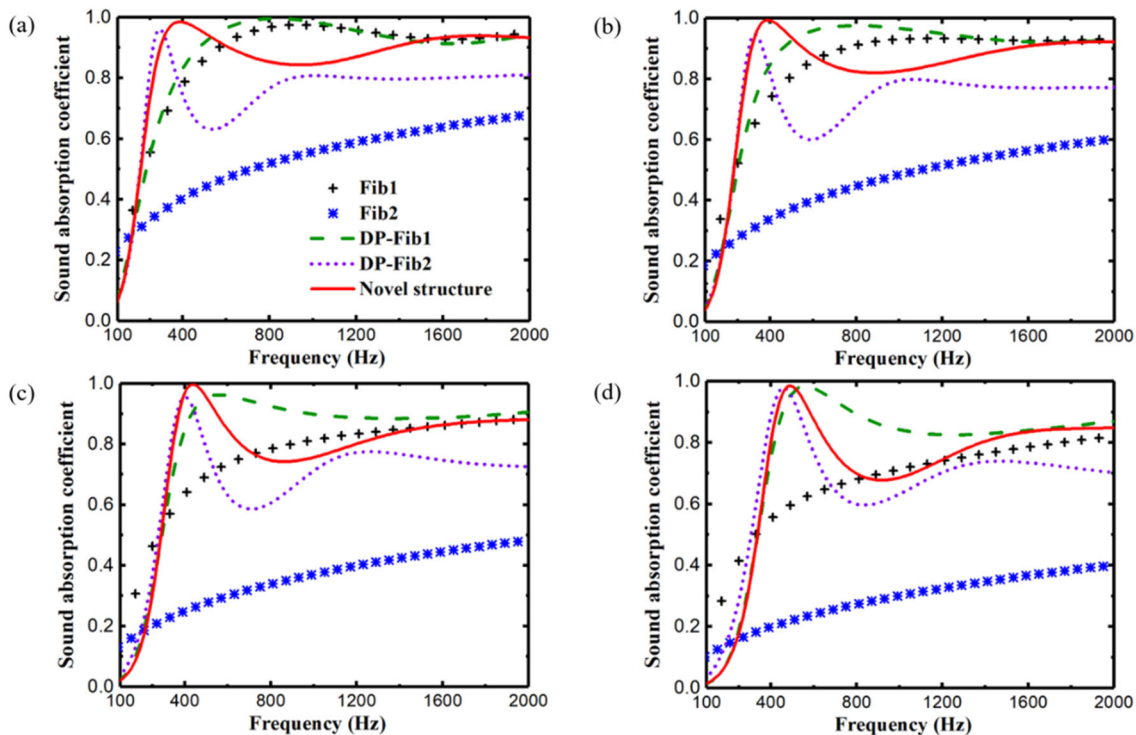
Fig. 3. Comparison of the sound absorption coefficients: **a** $t = 20°\text{C}$; **b** $t = 100°\text{C}$; **c** $t = 300°\text{C}$; **d** $t = 500°\text{C}$

frequency compared with that for DP-Fib2, and it lies between the two corresponding frequencies for DP-Fib1 and DP-Fib2. Although a decrease of the peak position of the sound absorption coefficient for DP-Fib1 can be observed as temperature increases, it can only reach about 560 Hz at the lowest, which is still higher than that for the proposed porous metamaterial structure and the one for DP-Fib2. Figure 3 shows clearly that the proposed porous metamaterial structure exhibits an improved sound absorption capacity in the low-frequency range, while the pristine porous material Fib1 and the double porosity material DP-Fib1 perform better in the intermediate-frequency range, at least for the considered temperature interval.

In order to reveal the underlying sound energy absorption mechanism, the distributions of time-averaged power dissipation density inside the unit-cell of porous metamaterial structure are shown in Fig. 4. Five different frequencies are chosen, among which 390 Hz, 440 Hz, and 500 Hz are the sound absorption peak frequencies of the porous metamaterial structure at 100°C, 300°C and 500°C, respectively. The total energy dissipated in each constituent porous material consists of two parts: the energy dissipated through the viscous effects and that through the thermal effects, and they can be determined from the acoustic wave propagation analysis in an equivalent fluid [21]. As shown in Fig. 4, most of the energy is dissipated in the upper part of the inner porous interlayer Fib1 with a lower airflow resistivity, independent of the considered temperature. However, the porous matrix Fib2 becomes more involved in the energy dissipation as the frequency increases, and a concentration of the dissipated energy can always be observed at the interface of the two different porous materials near the top surface at 2000 Hz. Besides it can be seen that the energy dissipation is minimal at 1000 Hz for all four considered temperatures, which corresponds to the trough of the sound absorption coefficient curves in Fig. 2 approximately.

Besides the distribution of the time-averaged power dissipation density inside the unit-cell of the porous metamaterial structure, the curves of the energy dissipation ratio at the four selected temperatures are also plotted in Fig. 5 to understand the role of each constituent porous material in the sound energy absorption process. The curves in Fig. 5 represent the proportion of the energy dissipated in each constituent porous material to the total energy dissipated inside the whole unit-cell of the porous
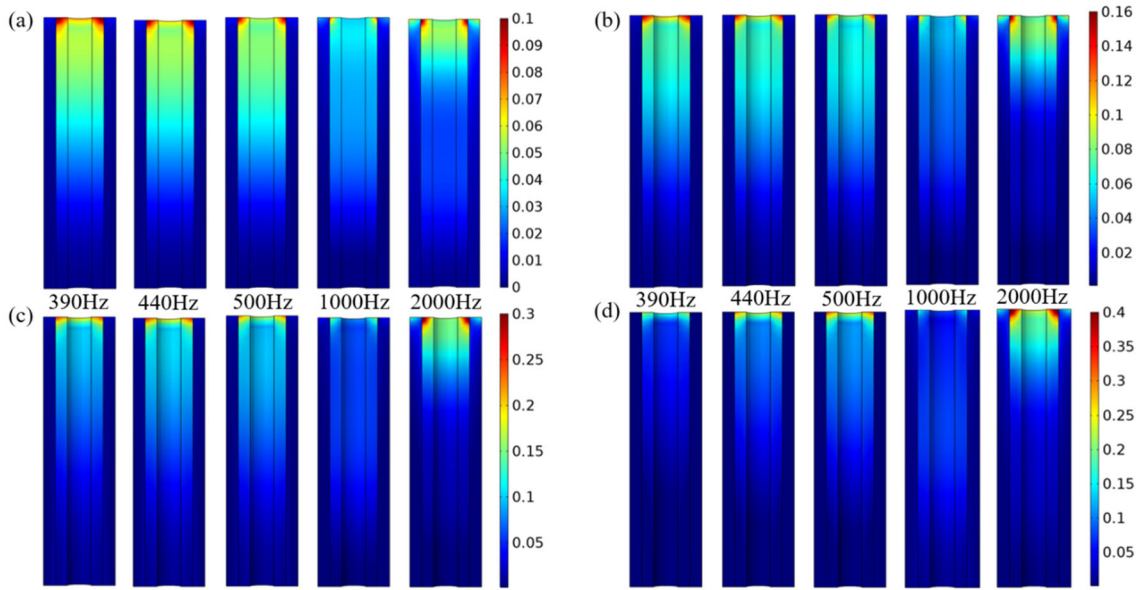
Fig. 4. Time-averaged power dissipation density (unit: W/m^3) in a unit-cell of the porous metamaterial structure: **a** $t = 20\,^\circ$C; **b** $t = 100\,^\circ$C; **c** $t = 300\,^\circ$C; **d** $t = 500\,^\circ$C
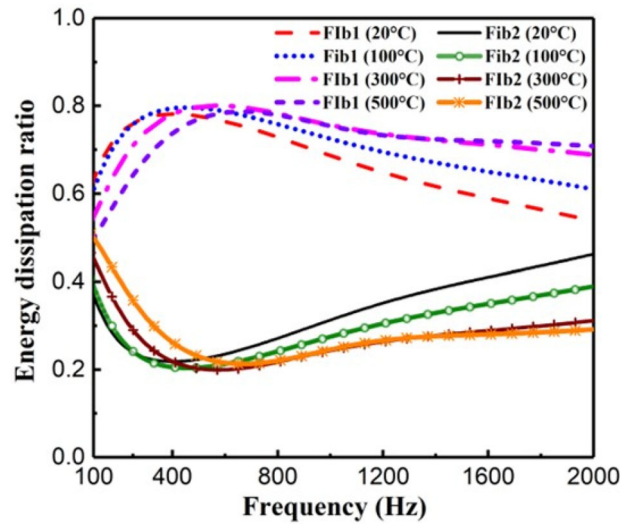

Fig. 5. Energy dissipation ratio of the two constituent porous materials at different temperatures

metamaterial structure. It can be seen here that regardless of the temperature, most of the energy is dissipated in the interlayer Fib1 as the ratio is always higher than 0.5. For all four considered temperatures, the energy dissipated in the interlayer Fib1 first increases and the maximum ratio is around 0.8 which indicates that about 80% of the total dissipated energy is dissipated in the interlayer Fib1. However, the energy dissipated in the interlayer Fib1 is reduced at intermediate and high frequencies, while the curves for the porous matrix Fib2 show an opposite trend. In a word, in the considered frequency range, the porous material with a lower airflow resistivity (Fib1) contributes more to the energy dissipation regardless of the temperature, while the contribution of the porous material with a higher airflow resistivity (Fib2) also becomes more remarkable at intermediate to high frequencies.

5. Conclusions

In this paper, a novel porous metamaterial structure with a superior high-temperature acoustic or sound energy absorption performance in the low-frequency range is presented. The proposed novel porous metamaterial structure consists of a porous material as matrix, periodically perforated cylindrical holes in a triangular lattice pattern, and another porous material as interlayers between the matrix and the perforated cylindrical holes. The double porosity theory is adopted to homogenize the interlayer and the cylindrical hole in a unit-cell as an equivalent acoustic inclusion, which is embedded in a porous matrix. Then, the porous matrix and the acoustic inclusion are further homogenized to build the theoretical model for the novel porous metamaterial structure. The variations of the relevant air and material parameters with temperature are taken into consideration in the extended theoretical model. To validate the established theoretical model, numerical simulations based on the FE model are performed, and fairly good agreement between the theoretically predicted and numerically computed results is achieved. The present results demonstrate that the proposed novel porous metamaterial structure exhibits a superior high-temperature acoustic energy absorption performance at low frequencies and in a rather wide frequency range. To explore and understand the underlying acoustic energy absorption mechanism inside the unit-cell of the porous metamaterial structure, the distribution of the time-averaged power dissipation density in the unit-cell as well as the energy dissipation ratio of each constituent porous material at different temperatures is also investigated in details. It is found that the two constituent porous materials contribute distinctively to the energy dissipation in different frequency ranges, and most of the energy is dissipated in the porous material with a lower airflow resistivity regardless of the temperature. The novel porous metamaterial structure proposed in this paper can be further optimized and utilized for efficiently absorbing the acoustic or sound energy at low frequencies and in high-temperature environments, which has important applications for noise reduction and insulation in mechanical and aerospace engineering.

References

[1] Huang X, Lu G, Yu TX. Energy absorption in splitting square metal tubes. Thin-Walled Struct. 2002;40:153–65.

[2] Su XY, Yu TX, Reid SR. Inertia-sensitive impact energy-absorbing structures, Part I: effects of inertia and elasticity. Int J Impact Eng. 1995;16:651–72.

[3] Su XY, Yu TX, Reid SR. Inertia-sensitive impact energy-absorbing structures, Part II: Effect of strain rate. Int J Impact Eng. 1995;16:673–89.

[4] Lu G, Yu TX. Energy Absorption of Structures and Materials. Amsterdam: Elsevier; 2003.

[5] Worraker WJ, Halliwell NA. Jet engine liner impedance: an experimental investigation of cavity neck flow/acoustics in the presence of a Mach 0.5 tangential shear flow. J Sound Vib. 1985;103:573–92.

[6] Zigoneanu L, Popa BI, Cummer SA. Three-dimensional broadband omnidirectional acoustic ground cloak. Nat Mater. 2014;13:352–5.

[7] Jiang X, Liang B, Li RQ, Zou XY, Ll Yin, Cheng JC. Ultra-broadband absorption by acoustic metamaterials. Appl Phys Lett. 2014;105:243505.

[8] Romero-Garcia V, Hladky-Hennion AC. Fundamentals and Applications of Acoustic Metamaterials: From Seismic to Radio Frequency. New York: Wiley; 2019.

[9] Deng J, Zheng L, Zeng P, Zuo Y, Guasch O. Passive constrained viscoelastic layers to improve the efficiency of truncated acoustic black holes in beams. Mech Syst Signal Process. 2019;118:461–76.

[10] Deng J, Guasch O, Zheng L. Ring-shaped acoustic black holes for broadband vibration isolation in plates. J Sound Vib. 2019;458:109–22.

[11] Deng J, Guasch O, Maxit L, Zheng L. Transmission loss of plates with multiple embedded acoustic black holes using statistical modal energy distribution analysis. Mech Syst Signal Process. 2021. https://doi.org/10.1016/j.ymssp.2020.107262.

[12] Gao N, Guo X, Deng J, Cheng B, Hou H. Elastic wave modulation of double-leaf ABH beam embedded mass oscillator. Applied Acoustics. 2021. https://doi.org/10.1016/j.apacoust.2020.107694.

[13] Zwikker C, Kosten CW. Sound Absorbing Materials. New York, 1949

[14] Delany M, Bazley E. Acoustical properties of fibrous absorbent materials. Applied Acoustics. 1970;3:105–16.

[15] Miki Y. Acoustical properties of porous materials–modifications of Delany-Bazley models. J Acoust Soc Japan. 1990;11:19–24.

[16] Johnson DL, Koplik J, Dashen R. Theory of dynamic permeability and tortuosity in fluid-saturated porous media. J Fluid Mech. 1987;176:379–402.

[17] Champoux Y, Allard JF. Dynamic tortuosity and bulk modulus in air-saturated porous media. J Appl Phys. 1991;70:1975–9.

[18] Pride SR, Morgan FD, Gangi AF. Drag forces of porous-medium acoustics. Phys Rev B. 1993;47:4964–78.

[19] Lafarge D, Lemarinier P, Allard JF, Tarnow V. Dynamic compressibility of air in porous structures at audible frequencies. J Acoust Soc Am. 1997;102:1995–2006.

[20] Sánchez-Palencia E. Non-Homogeneous Media and Vibration Theory. Berlin, West Germany: Spring-Verlag; 1980. p. 127.

[21] Atalla N, Panneton R, Sgard FC, Olny X. Acoustic absorption of macro-perforated porous materials. J Sound Vib. 2001;243:659–78.

[22] Olny X, Boutin C. Acoustic wave propagation in double porosity media. J Acoust Soc Am. 2003;114:73–89.

[23] Sgard FC, Olny X, Atalla N, Castel F. On the use of perforations to improve the sound absorption of porous materials. Appl Acoust. 2005;66:625–51.

[24] Ren SW, Meng H, Xin FX, Lu TJ. Ultrathin multi-slit metamaterial as excellent sound absorber: influence of micro-structure. J Appl Phys. 2016;119:014901.

[25] Ren SW, Meng H, Xin FX, Lu TJ. Sound absorption enhancement by thin multi-slit hybrid structures. Chinese Phys Lett. 2015;32:014302.

[26] Xin F, Ma X, Liu X, Zhang C. A multiscale theoretical approach for the sound absorption of slit-perforated double porosity materials. Compos Struct. 2019;223:110919.

[27] Gourdon E, Seppi M. On the use of porous inclusions to improve the acoustical response of porous materials: analytical model and experimental verification. Appl Acoust. 2010;71:283–98.

[28] Groby JP, Wirgin A, De Ryck L, Lauriks W, Gilbert RP, Xu YS. Acoustic response of a rigid-frame porous medium plate with a periodic set of inclusions. J Acoust Soc Am. 2009;126:685–93.

[29] Chevillotte F, Jaouen L, Bécot FX. On the modeling of visco-thermal dissipations in heterogeneous porous media. J Acoust Soc Am. 2015;138:3922–9.

[30] Gao N, Tang L, Deng J, Lu K, Hou H, Chen K. Design, fabrication and sound absorption test of composite porous metamaterial with embedding I-plates into porous polyurethane sponge. Appl Acoust. 2021;175:107845.

[31] Giese F, Ries HC, Eigenbrod C. On the performance of porous sound absorbent material in high temperature applications. J Eng Gas Turbines Power. 2010;132:121301.

[32] Christie DRA. Measurement of the acoustic properties of a sound absorbing material at high temperatures. J Sound Vib. 1976;46:347–55.

[33] Williams PT, Kirby R, Malecki C, Hill J. Measurement of the bulk acoustic properties of fibrous materials at high temperatures. Appl Acoust. 2014;77:29–36.

[34] Sun F, Chen H, Wu J, Feng K. Sound absorbing characteristics of fibrous metal materials at high temperatures. Appl Acoust. 2010;71:221–35.

[35] Ren S, Xin F, Lu TJ, Zhang C. A semi-analytical model for the influence of temperature on sound propagation in sintered metal fiber materials. Mater Design. 2017;134:513–22.

[36] Leclaire P, Kelders L, Lauriks W, Melon M, Brown N, Castagnède B. Determination of the viscous and thermal characteristic lengths of plastic foams by ultrasonic measurements in helium and air. J Appl Phys. 1996;80:2009–12.

[37] Panneton R, Olny X. Acoustical determination of the parameters governing viscous dissipation in porous media. J Acoust Soc Am. 2006;119:2027–40.

[38] Olny X, Panneton R, Tran-Van J. An indirect acoustical method for determining intrinsic parameters of porous materials. Poromechanics II. Boca Raton: CRC Press; 2020.

[39] Tarnow V. Airflow resistivity of models of fibrous acoustic materials. J Acoust Soc Am. 1996;100:3706–13.

[40] Allard J, Atalla N. Propagation of Sound in Porous Media: Modelling Sound Absorbing Materials. 2nd ed. United Kingdom: Wiley; 2009.

[41] Jia X, Yan M, Hong M. Sound energy enhancement via impedance-matched anisotropic metamaterial. Mater Design. 2021;197:109254.